

Frequency Domain Detectors in Different Short-Range Ultra-Wideband Communication Scenarios

Tiziano Bianchi and Simone Morosi

Dipartimento di Elettronica e Telecomunicazioni, Università degli Studi di Firenze, Via S. Marta 3, 50139 Firenze, Italy

Received 2 September 2005; Revised 26 May 2006; Accepted 3 November 2006

We study the performance of an innovative communication scheme for ultra-wideband systems which are based on impulse radio in two different short-range communication scenarios: the proposed system relies on both the introduction of the cyclic prefix at the transmitter and the use of a frequency domain detector at the receiver. Two different detection strategies based either on the zero forcing (ZF) or on the minimum mean square error (MMSE) criteria have been investigated and compared with the classical RAKE, considering two scenarios where a base station transmits with a different data rate to several mobile terminals in an indoor environment characterized by severe multipath propagation. The results show that the MMSE receiver achieves a remarkable performance, especially in the case of highly loaded high data-rate systems. Hence, the proposed approach is well suited for high-throughput applications in indoor wireless environments where multipath propagation tends to increase the effects of the interference.

Copyright © 2006 T. Bianchi and S. Morosi. This is an open access article distributed under the Creative Commons Attribution License, which permits unrestricted use, distribution, and reproduction in any medium, provided the original work is properly cited.

1. INTRODUCTION

Different applications can be foreseen for the impulse radio (IR) communications [1], based on the use of baseband pulses of very short duration, typically on the order of a nanosecond [2]: in particular, low and high data-rate applications have been envisaged.

For what concerns low data-rate services, impulse radio can be considered as one of the most suitable technologies: the transmitter can be kept much simpler than with conventional narrowband systems, permitting extreme low energy consumption, and thus long-life battery-operated devices, which are mainly used in low data-rate networks with low duty cycles, such as surveillance of areas difficult to access by humans, collecting difficult-to-gather data, wireless body area networks (WBANs), which are envisaged for medical supervision. Moreover, the UWB inherent temporal resolution due to large bandwidth enables positioning with previously unattained precision, tracking, and distance measuring techniques, as well as accommodating high node densities due to the large operating bandwidth.

Within the context of high data rate, the main application areas include

- (i) internet access and multimedia services: very high data rates (up to 1 Gbit/s) will have to be provided either

due to high peak data rates (download activity, streaming video), or high numbers of users (lounges, cafés, etc.), or both;

- (ii) wireless peripheral interfaces: a growing number of devices (laptop, mobile phone, PDA, headset, etc.) will have to be interconnected. Standardized wireless interconnection is highly desirable to replace cables and proprietary plugs;
- (iii) location-based services: to supply the user with the information he/she currently needs, at any place and any time (e.g., location-aware services in museums or at exhibitions), the users' position has to be accurately measured.

It is well known that IR systems have been recently studied as one of the most interesting ultra-wideband (UWB) techniques [3]. IR multiuser communication systems rely on the use of time-hopping (TH) spread-spectrum signals and impulsive modulation techniques such as pulse position modulation (PPM) or antipodal modulation techniques such as binary pulse amplitude modulation (PAM) [1, 4, 5]. In these systems, the same symbol is repeated many times, according to a specific random code, thus providing a very high processing gain.

The multipath diversity inherent in the received IR signals and the high processing gain have led most of the

researchers to consider correlation or RAKE receivers as the most suitable solution for this kind of communications (see the references in [6]). Nevertheless, even if the transmitted signals can be assumed synchronous and coordinated, for example, when the downlink between the access point (AP) and the mobile terminals (MTs) is considered, a dense multipath channel may cause a remarkable level of inter-path interference (IPI). As a consequence, UWB communications are expected to show a considerable level of both self-interference and multiple-access interference (MAI), which severely limits the performance of RAKE receivers. It is important to stress that in these systems, also the power consumption issue plays an important role when subnanosecond pulses are taken into account.

A conventional antimultipath approach for a single-carrier transmission is the adaptive equalization at the receiver [7]: anyway, since adaptive equalizers require one or more filters for which the number of adaptive tap coefficients is on the order of the number of data samples spanned by the multipath, they are not suitable for UWB indoor communications where more than 100 channel resolvable replicas have to be taken into account.

Frequency domain equalization (FDE) [8], proposed and studied for a single-carrier single-user environment, is simply the frequency domain analog of conventional equalizer. Channel impairments due to severe multipath propagation can be effectively faced by the FDE approach which proves to be computationally simpler than the corresponding time domain processing.

In this paper, an original frequency domain detector (FDD) for UWB impulse radio (UWB-IR) short-range downlink communications will be proposed and simulated in an extremely frequency-selective environment [9], aiming at highlighting how the orthogonality loss and the rise of both self-interference and MAI can be effectively coped with. The proposed receiver is based on the use of an analog correlation as the front end, followed by an analog-to-digital converter (ADC) [10–12]: this hybrid architecture affords looser sampling rate requirements, for example, down to the inverse of the pulse duration, and permits less complex system implementations.

2. SIGNAL MODEL

2.1. Pulse position modulation

In a downlink UWB-IR communication system using PPM, the signal which is transmitted to the ℓ th user can be expressed as [4, 13]

$$s_\ell(t) = \sqrt{\frac{E_b}{N_f}} \sum_{m=-\infty}^{+\infty} w_{tx} \left(t - mT_f - c_\ell(m)T_c - \tau \left(b_\ell \left(\left\lfloor \frac{m}{N_f} \right\rfloor \right) \right) \right), \quad (1)$$

where $w_{tx}(t)$ indicates a transmit pulse waveform having unit energy, T_f and T_c are the frame and the chip periods, respectively, and $b_\ell(i) = \pm 1$ is the i th binary symbol transmitted to

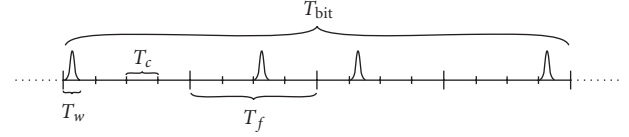


FIGURE 1: Representation of a transmitted bit. In the above example, $b = 1$ and $c_\ell(m) = \{0, 2, 1, 3\}$.

the ℓ th user. Since $\lfloor x \rfloor$ stands for the integer part of x , (1) indicates that a single bit is transmitted with energy E_b by the repetition of N_f pulses each belonging to a different frame period. We assume that N_c chips exactly fit in one frame period, that is, $T_f = N_c T_c$. Each active user is associated with a time-hopping pattern $c_\ell(m)$, which is modeled as a periodic pseudorandom sequence with period N_f . Finally, $\tau(b)$ indicates the additional pulse shift that implements PPM. In the binary case, we have $\tau(b) = \{0, T_w\}$ depending on $b = \{1, -1\}$, where $T_w^{\text{PPM}} = T_c/2$ represents the minimum sampling interval. An example of a transmitted bit is shown in Figure 1.

2.2. Pulse amplitude modulation

When a PAM is considered, the signal which is transmitted to the ℓ th user can be expressed as [14]

$$s_\ell(t) = \sqrt{\frac{E_b}{N_f}} \sum_{m=-\infty}^{+\infty} w_{tx}(t - mT_f - c_\ell(m)T_c) d_\ell(m) b_\ell \left(\left\lfloor \frac{m}{N_f} \right\rfloor \right), \quad (2)$$

where the involved quantities can be defined in an analogous way as in (1). In particular, $d_\ell(m)$ is used to distinguish between two types of UWB-IR PAM systems. In the first type, $d_\ell(m) = 1$ for each (ℓ, m) , whereas in the second one $d_\ell(m)$ are binary random variables, independent for $(\ell_1, m_1) \neq (\ell_2, m_2)$, and taking value ± 1 with equal probability. The first type of system can be considered the PAM counterpart of the system in (1) and will be simply referred to as PAM, while the second one employs a pulse-based polarity randomization (PR) [14] and will be referred to as PR-PAM. Note that in both cases, the minimum sampling interval is $T_w^{\text{PAM}} = T_c$, since there is only one pulse position inside a chip period.

2.3. Digital representation

In order to obtain a convenient representation for PPM, PAM, and PR-PAM IR-UWB, the transmitted signal can be represented as

$$s_\ell(t) = \sum_{k=-\infty}^{+\infty} w_{tx}(t - kT_w) \left[q_\ell(k) b_\ell \left(\left\lfloor \frac{k}{N_w} \right\rfloor \right) + p_\ell(k) \right], \quad (3)$$

where $q_\ell(k)$ and $p_\ell(k)$ are suitable sequences.

In the case of PPM, such sequences can be defined as

$$q_\ell(k) = \begin{cases} \sqrt{\frac{E_b}{4N_f}} & \text{if } k = 2[mN_c + c_\ell(m)], \\ -\sqrt{\frac{E_b}{4N_f}} & \text{if } k = 2[mN_c + c_\ell(m)] + 1, \\ 0 & \text{elsewhere,} \end{cases} \quad (4)$$

$$p_\ell(k) = |q_\ell(k)|,$$

where m denotes any integer value. For their definition and the properties of $c_\ell(m)$, both $q_\ell(k)$ and $p_\ell(k)$ are periodic with period equal to $N_w^{\text{PPM}} = 2N_cN_f$.

In the case of both PAM and PR-PAM, the above sequences can be redefined as

$$q_\ell(k) = \begin{cases} d_\ell(m) \sqrt{\frac{E_b}{N_f}} & \text{if } k = mN_c + c_\ell(m), \\ 0 & \text{elsewhere,} \end{cases} \quad (5)$$

$$p_\ell(k) = 0 \quad \text{for each } k.$$

In this case, both $q_\ell(k)$ and $p_\ell(k)$ are periodic with period equal to $N_w^{\text{PAM}} = N_cN_f$.

If we consider a base station which transmits synchronously to a set of N_u active users $I_u = \{\ell_1, \ell_2, \dots, \ell_{N_u}\}$, the signal which is transmitted by the base station is given by $s(t) = \sum_{\ell \in I_u} s_\ell(t)$ and the received signal after matched filtering can be expressed as

$$r(t) = w_{rx}(t) * g(t) * s(t) + n(t), \quad (6)$$

where $w_{rx}(t)$ is the impulse response of the filter matched to the received pulse waveform, $g(t)$ models the effects of both the antennas and the multipath channel, $*$ indicates convolution, and $n(t)$ models the thermal noise. Hence, recalling (3), we can express the received waveform as

$$r(t) = \sum_{k=-\infty}^{+\infty} \phi(t - kT_w) \sum_{\ell \in I_u} x_\ell(k) + n(t), \quad (7)$$

where $\phi(t) = w_{rx}(t) * g(t) * w_{tx}(t)$ and we define $x_\ell(k) = [q_\ell(k)b_\ell(\lfloor k/N_w \rfloor) + p_\ell(k)]$. By assuming that the channel characteristics are constant over the entire block of samples and sampling $r(t)$ with period T_w , we obtain the digital transmission model as

$$y(n) \triangleq r(nT_w) = \sum_{k=-\infty}^{+\infty} h(n-k) \sum_{\ell \in I_u} x_\ell(k) + e(n), \quad (8)$$

where $h(n) \triangleq \phi(nT_w)$ represents the equivalent discrete-time channel impulse response of the UWB-IR system and $e(n) \triangleq n(nT_w)$.

3. SYSTEM REPRESENTATION

In order to provide a description of the proposed approach, a block vectorial representation of the above described model is more convenient. Moreover, such a representation allows us to effectively introduce the concept of low data-rate and high data-rate services into the considered system.

3.1. Block representation of low data-rate and high data-rate scenarios

Let us subdivide the discrete signal $x_\ell(n)$ in blocks of M samples. We define the vector $\mathbf{x}_\ell(i) = [x_\ell(iM), x_\ell(iM+1), \dots, x_\ell(iM+M-1)]^T$, consisting of the samples of the signals transmitted by the ℓ th user.

In order to perform FDE [8], each block is extended by means of a cyclic prefix (CP) of length K , that is, the last K samples of the block are repeated at the beginning of the block. One of the crucial issues in the FD receiver design is the selection of a convenient value of the parameters K and M , which determine both the overhead in terms of redundant samples and the computational complexity of the receiver.

In this paper, the redundancy due to the CP approach is not considered as an overhead, but as an alternative to the processing gain N_f . If we assume that the CP size K has been fixed, the minimum block size required by FD equalization is $M \geq K$. In traditional CP-based systems, in order to achieve a tradeoff between the complexity burden and the redundancy due to CP insertion, the block size is usually chosen so as to have $4K \leq M \leq 8K$. However, this requisite is not strictly necessary for UWB, since this kind of systems usually allows for redundancy in terms of pulse repetition. Hence, it is convenient to set the block size as small as possible, so reducing the complexity of the FD equalization, and to compensate for the loss of throughput by shortening the pulse repetition factor N_f .

In the following, the block size is set to $M = K$. Therefore, in order to have the same rate of the original system, the repetition factor of the FD system is set to $N_f^{\text{CP}} = N_f/2$. We point out that this choice does not impose any particular relationship between the values of M and the number of samples $N_w^{\text{CP}} = N_w/2$ that are associated with a single bit. In general, we can have either situations in which $M < N_w^{\text{CP}}$, that is, the same bit is transmitted by more than one block (low data-rate scenario), or situations in which $M \geq N_w^{\text{CP}}$, that is, one or more bits are transmitted in a single block (high data-rate scenario). However, for the sake of simplicity, in the following we will consider only systems in which either $M = N_w^{\text{CP}}/N_M$, that is, we need exactly N_M blocks to transmit a single bit, or $M = N_b N_w^{\text{CP}}$, that is, a group of N_b bits is exactly spread over a block of M samples.

In the first case, the expression of $\mathbf{x}_\ell(i)$ is given as

$$\mathbf{x}_\ell(i) = b_\ell \left(\left\lfloor \frac{i}{N_M} \right\rfloor \right) \mathbf{q}_\ell^{(i)} + \mathbf{p}_\ell^{(i)}, \quad (9)$$

where $\mathbf{q}_\ell^{(i)} = [q_\ell(iN_M), \dots, q_\ell(iN_M + N_M - 1)]^T$ and $\mathbf{p}_\ell^{(i)} = [p_\ell(iN_M), \dots, p_\ell(iN_M + N_M - 1)]^T$.

In the second case, we can express $\mathbf{x}_\ell(i)$ as

$$\mathbf{x}_\ell(i) = [b_\ell(iN_b) \mathbf{q}_\ell^T + \mathbf{p}_\ell^T, \dots, b_\ell(iN_b + N_b - 1) \mathbf{q}_\ell^T + \mathbf{p}_\ell^T]^T, \quad (10)$$

where $\mathbf{q}_\ell = [q_\ell(0), q_\ell(1), \dots, q_\ell(N_w - 1)]^T$ and $\mathbf{p}_\ell = [p_\ell(0), p_\ell(1), \dots, p_\ell(N_w - 1)]^T$. If we define the vector of the bits

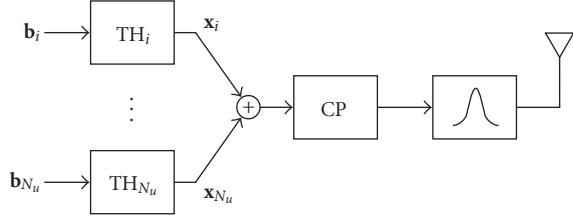


FIGURE 2: Block representation of the BT UWB-IR transmitter with cyclic prefix.

transmitted to the ℓ th user in the i th block as $\mathbf{b}_\ell(i) = [b_\ell(iN_b), b_\ell(iN_b+1), \dots, b_\ell(iN_b + N_b - 1)]^T$, (10) can be rewritten in a more compact form as

$$\mathbf{x}_\ell(i) = \mathcal{Q}_{\ell,M} \mathbf{b}_\ell(i) + \mathbf{p}_{\ell,M}, \quad (11)$$

where $\mathcal{Q}_{\ell,M} = \mathbf{I}_{N_b} \otimes \mathbf{q}_\ell$, $\mathbf{p}_{\ell,M} = \mathbf{1}_{N_b} \otimes \mathbf{p}_\ell$, \otimes indicates Kronecker product, and $\mathbf{1}_{N_b}$ is an all-ones column vector of size N_b . The block representation of the UWB-IR transmitter is shown in Figure 2.

3.2. Channel representation

In both scenarios, if $K \geq L_c$, where L_c indicates the number of the channel resolvable replicas, there is no interference between adjacent blocks, and the effect of UWB-IR channel can be modeled as a circular convolution between the channel impulse response and the block of M samples. Hence, if we define the received vector after cyclic prefix removal as $\mathbf{y}(i) = [y(iM), y(iM+1), \dots, y(iM+M-1)]^T$, then the input-output relation of the UWB-IR system with cyclic prefix can be expressed as

$$\mathbf{y}(i) = \mathcal{H} \sum_{\ell \in I_u} \mathbf{x}_\ell(i) + \mathbf{e}(i), \quad (12)$$

where \mathcal{H} models channel effects and $\mathbf{e}(i) = [e(iM), e(iM+1), \dots, e(iM+M-1)]^T$.

4. RECEIVER SCHEMES

4.1. RAKE

The RAKE receiver, which relies on the correlation with delayed replicas of a template waveform [4, 15], has been proposed for UWB-IR systems both for its ability in exploiting the multipath diversity as well as for its low complexity. If we apply the maximum ratio combining (MRC) algorithm, the decision variable of the ℓ th user can be expressed as

$$v_\ell^{\text{RAKE}}(i) = \sum_{k \in I_{rp}} h^*(k) z_\ell(i, k), \quad (13)$$

where I_{rp} indicates the set of the resolvable channel paths and $z_\ell(i, k)$ is the output of the k th finger.

of the k th finger is given by

$$\begin{aligned} z_\ell(i, k) &= \sum_{h=0}^{N_f-1} [y(2(N_c(iN_f + h) + c_\ell(h) + k) \\ &\quad - y(2(N_c(iN_f + h) + c_\ell(h)) + k + 1))] \end{aligned} \quad (14)$$

while for both PAM and PR-PAM, the output of the k th finger is

$$z_\ell(i, k) = \sum_{h=0}^{N_f-1} y(N_c(iN_f + h) + c_\ell(h) + k). \quad (15)$$

Finally, the sign of the decision variable determines the value of the bit received by the ℓ th user.

4.2. Frequency domain detection

Channel equalization in the frequency domain [8] is a possible solution to the IPI which is caused by the autocorrelation functions of the time-hopping sequences. Consider the block model in (12). Since matrix \mathcal{H} is circulant, it can be diagonalized by using a discrete Fourier transform (DFT) as $\mathcal{H} = \mathbf{W}_M^H \mathbf{\Lambda}_{\mathcal{H}} \mathbf{W}_M$, where \mathbf{W}_M is an $M \times M$ Fourier transform matrix and $\mathbf{\Lambda}_{\mathcal{H}}$ is an $M \times M$ diagonal matrix whose entries represent the channel frequency response.

Frequency domain detection is performed in the following steps. First, we take the DFT of the received vector $\mathbf{y}(i)$. Then, the effect of the channel is compensated by taking into account the frequency response $\mathbf{\Lambda}_{\mathcal{H}}$. Finally, the signal is brought back to its time representation by means of an IDFT and the decision is made by taking the correlation between the received signal and the time-hopping sequence of the desired user. In matrix notation, the decision variables when $M < N_w$ and $M \geq N_w$ can be expressed as

$$v_\ell(r) = \sum_{i=rN_M}^{rN_M+N_M-1} \mathbf{q}_\ell^{(i),T} \mathbf{W}_M^H \mathcal{D} \mathbf{W}_M \mathbf{y}(i), \quad (16)$$

$$\mathbf{v}_\ell(i) = \mathcal{Q}_{\ell,M}^T \mathbf{W}_M^H \mathcal{D} \mathbf{W}_M \mathbf{y}(i),$$

respectively, where \mathcal{D} represents the frequency domain equalization.

In this paper, we will focus on two linear receiver techniques, namely zero-forcing (ZF) and minimum mean-square error (MMSE) equalizations, due to their good trade-off between performance and complexity. The ZF detector is implemented by letting \mathcal{D} equal to the inverse of channel's frequency response, that is,

$$\mathcal{D}^{\text{ZF}} = \mathbf{\Lambda}_{\mathcal{H}}^{-1}. \quad (17)$$

In this case, the effect of channel is exactly compensated and self-interference is totally avoided. Moreover, if we use orthogonal time-hopping sequences, also MAI can be completely eliminated. Nevertheless, it is well known that this solution amplifies the noise at the receiver, and hence a performance degradation for low SNR values is expected.

The expression of \mathcal{D} for the MMSE detector is given by

$$\mathcal{D}^{\text{MMSE}} = \Lambda_{\mathcal{H}}^H \left(\Lambda_{\mathcal{H}} \Lambda_{\mathcal{H}}^H + \frac{N_w \sigma_e^2}{N_u \sigma_b^2} \mathbf{I}_M \right)^{-1}, \quad (18)$$

where σ_e^2 is the noise variance and σ_b^2 indicates the power of transmitted symbols. This solution avoids noise amplification at the detector when the SNR is low. However, it requires the knowledge of both the noise variance and the power of transmitted symbols, as well as the number of active users. Particularly, the MMSE detector relies on the approximation $\mathbf{C}_{\mathbf{x}\mathbf{x}} \approx N_u \sigma_b^2 / N_w \mathbf{I}_M$, where $\mathbf{C}_{\mathbf{x}\mathbf{x}}$ is the autocorrelation matrix of the overall transmitted signal $\mathbf{x} = \sum_{\ell} \mathbf{x}_{\ell}$. Actually, this assumption does not hold due to the pulse repetition, but it allows us to derive a diagonal $\mathcal{D}^{\text{MMSE}}$. Moreover, the MMSE detector (18) does not require any knowledge of the time-hopping sequences of the interfering users. Therefore, the solution in (18) can be thought as a suboptimal MMSE receiver requiring a quite limited complexity.

5. SIMULATION RESULTS

The performance of the proposed systems has been verified by simulating a UWB-IR link between an AP transmitting to a variable number of MTs and a reference MT. The information bits are modulated by means of either a 2-PPM or a 2-PAM. Orthogonal time-hopping sequences are used, so that we can allocate up to N_c orthogonal users. Since they are transmitted from the same AP, all the users can be assumed synchronous. The pulse duration is equal to $T_w = 2$ nanoseconds. Two simulation scenarios have been considered, which are characterized by different values of the data rate. In the high data-rate case, the bits are repeated over $N_f = 4$ frames each consisting of either $N_c = 4$ (PPM) or $N_c = 8$ (PAM) chips, resulting in an uncoded rate of about 15.6 Mbit/s. In the low data-rate scenario, N_f and N_c have been assumed equal to 64 and either 16 (PPM) or 32 (PAM), respectively, affording an uncoded rate of about 244 kbit/s. The two different values of N_c are employed to have the same rate for both PPM and PAM systems.

The channel has been simulated according to the model in [9], assuming a slow fading scenario. We also assumed a constant power delay profile with an rms delay spread of about 50 nanoseconds, which is a typical value for indoor environments. This resulted in a digital channel model having $L_{\text{RAKE}} = 100$ sample-spaced resolvable replicas. When using FDD, each block of $M = 128$ samples is extended by means of a cyclic prefix of 128 samples, so that the channel causes no interference between adjacent blocks. We note that in this case, the actual pulse repetition N_f is halved, so as to maintain the same redundancy as the systems without CP.

The bit error rate (BER) for the systems using RAKE receiver and the systems using FDD with ZF equalization (FDD-ZF) and MMSE equalization (FDD-MMSE) has been evaluated by averaging over 10000 independent channel realizations. For the systems using PAM, also pulse-based polarity randomization has been considered. The corresponding systems have been denoted as RAKE-PR and FDD-MMSE-

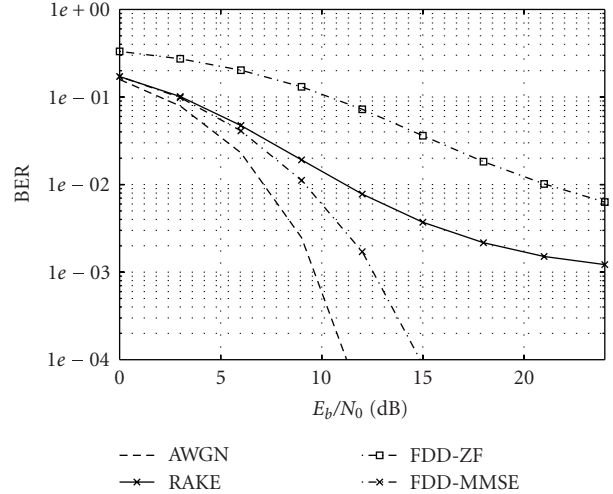


FIGURE 3: Performance comparison for PPM, $N_u = 1$ ($N_c = 4, N_f = 4$).

PR.¹ Finally, perfect knowledge of the channel parameters has been assumed.

In Figure 3, we show the comparison of BER performance versus E_b/N_0 ratio for a single user high data-rate PPM communication system: though no multiple-access interference has been introduced, the long delay spread of the multipath components causes a remarkable level of self-interference between the replicas of the signals; hence, the RAKE receiver’s performance is bounded by an irreducible error floor that is clearly visible for high values of E_b/N_0 ratio. On the other hand, even if FDD-ZF compensates channel effects, and, therefore, does not show any error floor, the noise enhancement caused by ZF equalization greatly impairs system performance with a loss of about 10 dB. As it can be clearly seen, FDD-MMSE proves to be the best solution since it does not increase the effects of thermal noise while suppressing self-interference and eliminating the error floor. We want to stress one more time that all these systems afford the same throughput due to the assumptions which have been made on the cyclic prefix and the repetition factor. If we consider a multiuser environment as in Figure 4, where UWB-IR systems with 2 and 4 users are simulated, the abilities of FDD-MMSE are even more evident. The RAKE receiver is not able to cope with MAI whose effects are increased by the long multipath spread: as a result, performance is greatly impaired and the error floor can be clearly seen also for medium to low E_b/N_0 values. On the contrary, both FDD strategies are able to restore the orthogonality between users since they perfectly compensate the effects of the channel, and the FDD-MMSE performance is only slightly degraded with respect to the single-user case.

¹ The FDD-ZF-PR system has not been considered here, since the use of orthogonal TH sequences together with a ZF approach allows us to remove all interference, thus making PR ineffective.

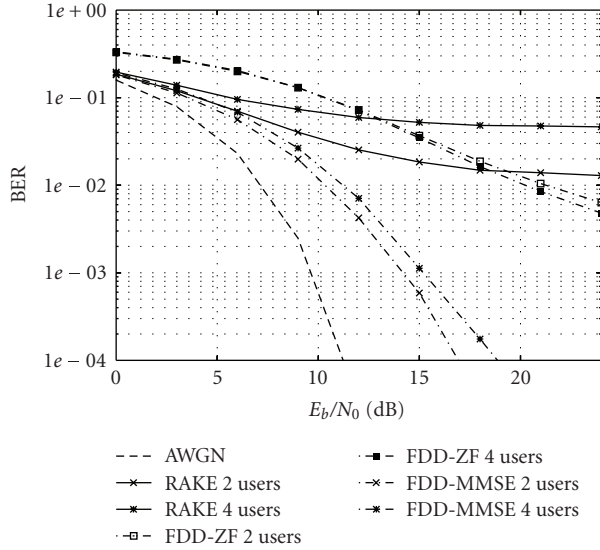


FIGURE 4: Performance comparison for PPM, $N_u = 2$ and $N_u = 4$ ($N_c = 4$, $N_f = 4$).

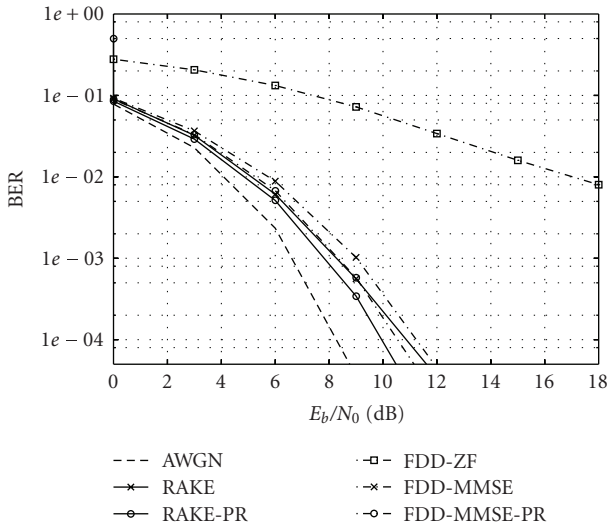


FIGURE 5: Performance comparison for PAM and PR-PAM, $N_u = 1$ ($N_c = 8$, $N_f = 4$).

In Figure 5, we consider the performance of the PAM and PR-PAM single-user high data-rate communication systems: the system throughput is the same as that of the previous simulation sets due to the assumptions on N_c . The abilities of the RAKE receiver in suppressing MAI and ISI are greatly increased by the adoption of the antipodal signaling and polarity randomization. As a result, the FDD-MMSE and RAKE performances are comparable. On the other hand, the results of the multiuser systems, reported in Figure 6, are more interesting: when the system load increases, the RAKE receiver performance is impaired by the MAI since no channel equalization helps in restoring user's orthogonality. Also the

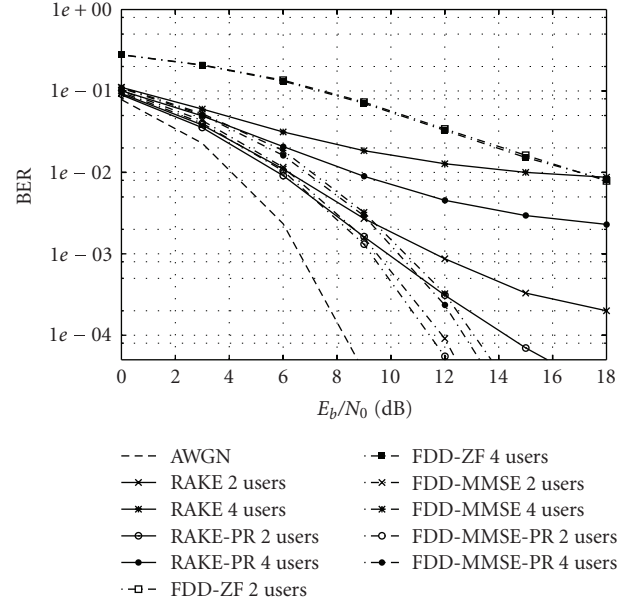


FIGURE 6: Performance comparison for PAM and PR-PAM, $N_u = 2$ and $N_u = 4$ ($N_c = 8$, $N_f = 4$).

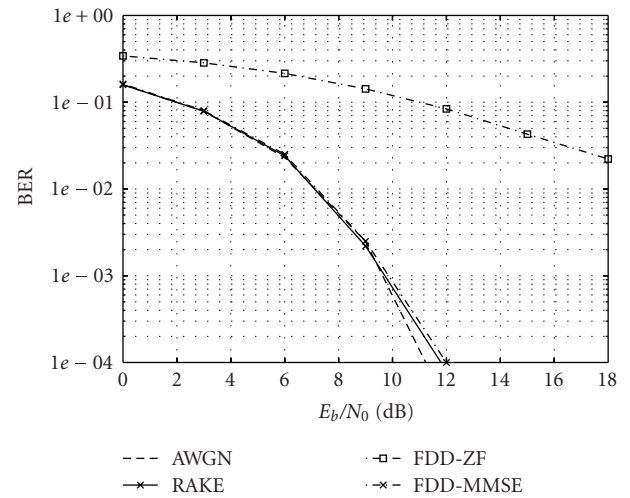


FIGURE 7: Performance comparison for PPM, $N_u = 1$ ($N_c = 16$, $N_f = 64$).

polarity randomization approach fails in suppressing the interference. The FDD-MMSE receiver, on the contrary, allows to preserve the separation of the users and affords a very good performance also in the fully loaded case.

For what concerns the low data-rate scenario, in Figure 7 the BER performance of the proposed receivers is reported for the single-user PPM case: the high value of the processing gain allows the RAKE receiver to efficiently face the ISI and to be very close to the AWGN bound. While the FDD-ZF performance is plagued as usual by the noise enhancement, the FDD-MMSE achieves a good performance which is nearly the same as that of the RAKE receiver. In Figure 8, we

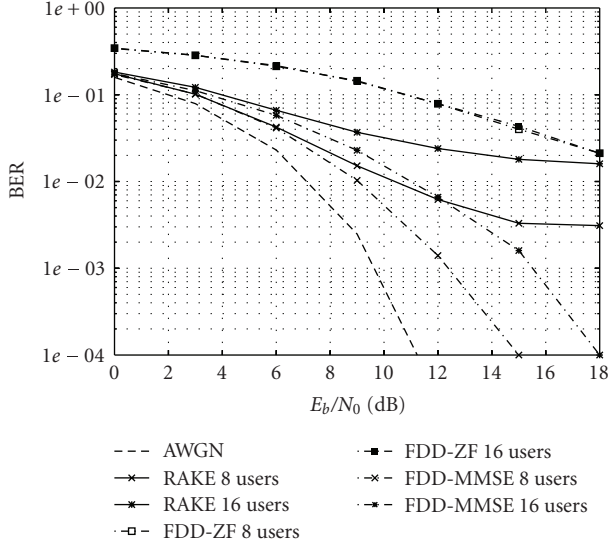


FIGURE 8: Performance comparison for PPM, $N_u = 8$ and $N_u = 16$ ($N_c = 16$, $N_f = 64$).

report the results of the proposed receiver for the low data-rate PPM multiuser environment: in particular, UWB-IR systems with 8 and 16 users are simulated which correspond to a half-loaded and a fully loaded system, respectively. While the RAKE receiver is impaired by the loss of orthogonality between the users due to the IPI, the FDD-MMSE receiver shows excellent MAI and self-interference suppression capabilities.

In Figure 9, the performance of the PAM and PR-PAM single-user low data-rate communication systems is reported: due to the high processing gain, the RAKE receiver achieves an almost ideal performance, while FDD-MMSE is characterized by a slightly worse result. If we consider the multiuser systems, reported in Figure 10, we can notice that the FDD-MMSE performance is better than the RAKE one when PAM signaling is adopted.

Conversely, the PR approach proves the most effective for the multiuser low data-rate system. The motivation of this behavior can be found in the great benefit which is caused by the polarity randomization in interference suppression. It is remarkable that also the performance of the FDD-MMSE receiver is sensibly improved by PR. This can be explained considering that the approximation of \mathbf{C}_{xx} used in the derivation of the FDD-MMSE receiver proves more tight when the polarity randomization is used.

We can conclude that the FDD-MMSE approach is very effective in highly loaded high data-rate scenarios, since such systems are more sensible to the effects of intersymbol interference and multiple-access interference. For these systems, either when PPM or PR-PAM signaling schemes are used, FDD-MMSE always achieves the best performance. On the other hand, the advantages of the FDD approach appear more limited in the case of low data-rate systems. For such systems, the effect of ISI is usually reduced by the long symbol period, and also the MAI is less harmful due to the

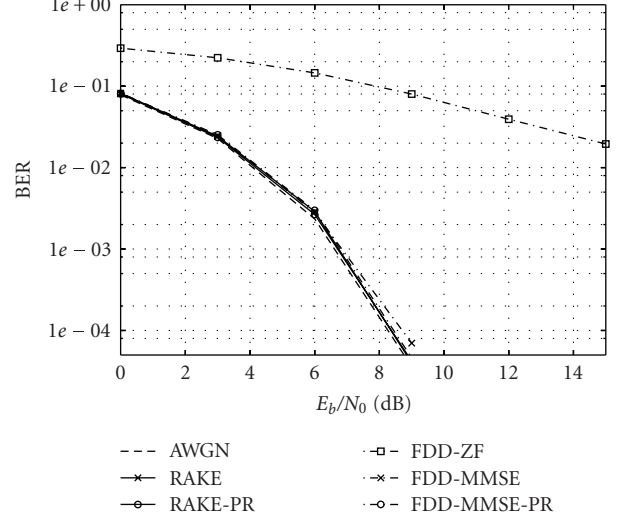


FIGURE 9: Performance comparison for PAM and PR-PAM, $N_u = 1$ ($N_c = 32$, $N_f = 64$).

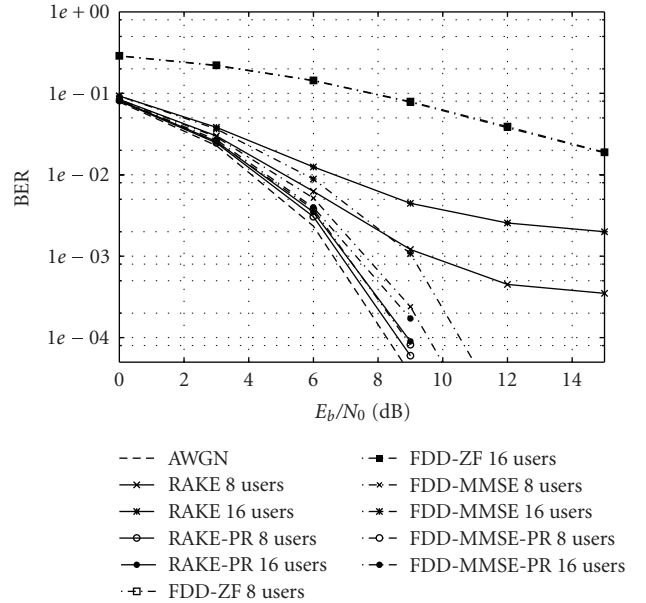


FIGURE 10: Performance comparison for PAM and PR-PAM, $N_u = 8$ and $N_u = 16$ ($N_c = 32$, $N_f = 64$).

increased processing gain. Moreover, the use of polarity randomization proves very beneficial in the case of a high processing gain, so that the performance of the FDD receiver is equal or slightly worse than that of the RAKE receiver with PR-PAM.

6. COMPLEXITY CONSIDERATIONS

For what concerns the complexity involved in the receivers which have been considered and tested, the RAKE receiver

appears to be the most simple since its computational load is proportional to the number of multipath components that have to be discerned in the receiver. Both FDD detectors are characterized by higher complexity, however, if we use a fast Fourier transform algorithm, the computational load of these detectors is proportional to the number of samples in the frame, that is, N_w : this value does not seem prohibitive for future implementations.

Also the performance of the analog-to-digital converter (ADC) has a deep impact on the choice of receiver architecture in a digital wireless system. In UWB systems, this phenomenon is enforced by the large operating bandwidth.

In IR-UWB systems, high-frequency A/D converters allow the implementation of correlation in the digital domain [11, 13] and enable new modulation and multiple-access concepts that exploit pulse shape. On the other hand, lower-frequency converters are based on the use of an analog correlation as a front end of the receiver: hence, in this hybrid architecture, the sampling rate requirement is relaxed which ensures the feasibility of digital radio for UWB systems [12].

Both solutions seem to have a promising future since they are particularly in line with the evolution of silicon technologies: as a matter of fact, digital/baseband circuits are implemented in CMOS. This technology offers excellent performance in terms of both power consumption and cost. At the same time, DSP-based designs also enjoy process portability, low sensitivity to component variability, as well as benefits from Moore's law. More specifically, a system design free of RF components will facilitate system-on-a-chip (SoC) implementation in CMOS, which shrinks as CMOS scales down from $0.18 \mu\text{m}$ to $0.13 \mu\text{m}$ and $0.09 \mu\text{m}$ [16].

The all-digital solution avoids analog delay lines but requires very high sampling rates in order to avoid aliasing: even if this solution is more attractive, it is not yet available off the shelf and needs further development. However, a massive research activity is focused on this issue also for the great interest which is currently spread over the software-defined radio (SDR) technologies: as it is known, the success of the SDR systems is strictly tied to the possibility to have simultaneous wideband and high-fidelity digitization.

On the contrary, the hybrid solution does not seem to be so far from reality: an outlook over the market allows to be optimistic about the feasibility of this receiver also in the near future: particularly, Analog Devices has launched the 12-bit 400 MSPS A/D Converter (AD12400), and has announced to be almost ready for the 500 MSPS. Therefore, it is likely that these solutions which are based on hybrid architecture will be used in the next years until the all-digital solution will become available on the market.

The proposed detector relies on a specific reception chain whose front end, after the receiving antenna, is composed by an analog correlator, namely a pulse deshaper, followed by an ADC which provides the samples to form the data blocks; however, the smallest time interval which is foreseen in the proposed system, that is, the pulse duration T_w , is equal to 2 nanoseconds. Therefore, in order to recover all the information, we only need to sample the output of the pulse correlator at 500 MSPS.

We are aware that such an architecture is less flexible and that the hybrid receiver will suffer from circuit mismatches and other nonidealities. The effects of these impairments on the performance of the proposed receiver can be taken into account by introducing more sophisticated channel and system models. However, this study is out of the scope of the present manuscript, which aims at presenting a new detection technique for IR-UWB systems which are based on a hybrid receiver, that is, an analog front end followed by an ADC.

7. CONCLUSIONS

In this paper, an innovative communication scheme for impulse radio ultra-wideband systems has been proposed. The proposed system is based on both the introduction of the cyclic prefix at the transmitter and the use of a frequency domain equalizer at the receiver. The frequency detection approach has been applied considering two different scenarios characterized by low data-rate and high data-rate services, respectively. Two different detection strategies based on either the ZF or the MMSE criteria have been investigated. The proposed detectors have been compared with the classical RAKE, considering a base station transmitting to several mobile terminals through a severe multipath channel. Simulation results have shown that both the FDD strategies are able to restore the orthogonality between users by compensating the effects of the channel. We found that the FDD-MMSE receiver achieves a remarkable performance for every configuration of active terminals. Moreover, the proposed receiver outperforms the RAKE receiver in the case of highly loaded high data-rate systems, so that it appears to be well suited for applications providing high data-rate services in the indoor wireless environment.

ACKNOWLEDGMENTS

This work has been partially supported by Italian Research Programs (PRIN 2005) "Situation and Location Aware Design Solutions over Heterogeneous Wireless Networks" and "Traffic and Terminal Self-Configuration in Integrated Mesh Optical and Broad Band Wireless Networks (TOWN)".

REFERENCES

- [1] M. Z. Win and R. A. Scholtz, "Impulse radio: how it works," *IEEE Communications Letters*, vol. 2, no. 2, pp. 36–38, 1998.
- [2] T. Brown, K. Schwiager, E. Zimmermann, et al., "Ultra wideband: technology and future perspectives," in *Proceedings of the 13th Wireless World Research Forum (WWRF '05)*, Jeju Island, Korea, March 2005, white paper.
- [3] D. Porcino and W. Hirt, "Ultra-wideband radio technology: potential and challenges ahead," *IEEE Communications Magazine*, vol. 41, no. 7, pp. 66–74, 2003.
- [4] M. Z. Win and R. A. Scholtz, "Ultra-wide bandwidth time-hopping spread-spectrum impulse radio for wireless multiple-access communications," *IEEE Transactions on Communications*, vol. 48, no. 4, pp. 679–691, 2000.

- [5] R. A. Scholtz, "Multiple access with time-hopping impulse modulation," in *Proceedings of IEEE Military Communications Conference (MILCOM '93)*, vol. 2, pp. 447–450, Boston, Mass, USA, October 1993.
- [6] J. D. Choi and W. E. Stark, "Performance of ultra-wideband communications with suboptimal receivers in multipath channels," *IEEE Journal on Selected Areas in Communications*, vol. 20, no. 9, pp. 1754–1766, 2002.
- [7] S. U. H. Qureshi, "Adaptive equalization," *Proceedings of the IEEE*, vol. 73, no. 9, pp. 1349–1387, 1985.
- [8] D. Falconer, S. L. Ariyavisitakul, A. Benyamin-Seeyar, and B. Eidson, "Frequency domain equalization for single-carrier broadband wireless systems," *IEEE Communications Magazine*, vol. 40, no. 4, pp. 58–66, 2002.
- [9] D. Cassioli, M. Z. Win, and A. F. Molisch, "The ultra-wide bandwidth indoor channel: from statistical model to simulations," *IEEE Journal on Selected Areas in Communications*, vol. 20, no. 6, pp. 1247–1257, 2002.
- [10] A. F. Molisch, Y. G. Li, Y.-P. Nakache, et al., "A low-cost time-hopping impulse radio system for high data rate transmission," *EURASIP Journal on Applied Signal Processing*, vol. 2005, no. 3, pp. 397–412, 2005.
- [11] W. Namgoong, "A channelized digital ultrawideband receiver," *IEEE Transactions on Wireless Communications*, vol. 2, no. 3, pp. 502–510, 2003.
- [12] R. Harjani, J. Harvey, and R. Sainati, "Analog/RF physical layer issues for UWB systems," in *Proceedings of the 17th IEEE International Conference on VLSI Design (VLSID '04)*, vol. 17, pp. 941–948, Mumbai, India, January 2004.
- [13] C. J. Le Martret and G. B. Giannakis, "All-digital impulse radio with multiuser detection for wireless cellular systems," *IEEE Transactions on Communications*, vol. 50, no. 9, pp. 1440–1450, 2002.
- [14] S. Gezici, H. Kobayashi, H. V. Poor, and A. F. Molisch, "Performance evaluation of impulse radio UWB systems with pulse-based polarity randomization," *IEEE Transactions on Signal Processing*, vol. 53, no. 7, pp. 2537–2549, 2005.
- [15] M. Z. Win and R. A. Scholtz, "On the robustness of ultra-wide bandwidth signals in dense multipath environments," *IEEE Communications Letters*, vol. 2, no. 2, pp. 51–53, 1998.
- [16] L. Yang and G. B. Giannakis, "Ultra-wideband communications: an idea whose time has come," *IEEE Signal Processing Magazine*, vol. 21, no. 6, pp. 26–54, 2004.

Simone Morosi was born in Firenze, Italy, in 1968. He received the Dr. Ing. degree in electronics engineering in 1996 and the Ph.D. degree in information and telecommunication engineering in 2000 from the University of Firenze, Firenze. Since 1999, he has been a Researcher of the Italian Interuniversity Consortium for Telecommunications (CNIT). Since 2000, he has been with the Department of Electronics and Telecommunications of the University of Firenze: currently he is a Research Assistant. His present research interests involve ultra-wideband systems, multiuser detection and turbo MUD techniques, MIMO systems. He has participated to several national research programs and to European Projects COST 262 and COST 273. He is currently participating in the European Networks of Excellence NEWCOM (Network of Excellence in Wireless COMMunications, 6th European Framework Program) and CRUISE (CReating Ubiquitous Intelligent Sensing Environments, 6th European Framework Program).



Tiziano Bianchi was born in Prato, Italy, in 1976. He received the M.S. degree (Laurea) in electronic engineering in 2001 and the Ph.D. degree in information and telecommunication engineering in 2005, both from the University of Firenze, Italy. From March 2005, he has been with the Department of Electronics and Telecommunications of the University of Florence as a Research Assistant. His research topics include signal processing in communications, ultra-wideband systems, and multicarrier modulation techniques, as well as wavelets and filterbanks theory, and applications of multirate systems. He is currently participating in the European Network of Excellence NEWCOM (Network of Excellence in Wireless COMMunications, 6th European Framework Program).

